NMR-based metabolomic analysis of the physiological role of the electron-bifurcating FeFehydrogenase Hnd in Solidesulfovibrio fructosivorans under pyruvate fermentation

Natalie Payne, Arlette Kpebe, Chloé Guendon, Carole Baffert, Matthieu Maillot, Typhaine Haurogné, Fabrice Tranchida, Myriam Brugna, Laetitia Shintu

NMR-based metabolomic analysis of the physiological role of the electron-bifurcating FeFe-hydrogenase Hnd in *Solidesulfovibrio fructosivorans* under pyruvate fermentation

Natalie Payne[1,3], Arlette Kpebe[1], Chloé Guendon[1], Carole Baffert[1], Matthieu Maillot[2], Typhaine Haurogné[2], Fabrice Tranchida[3], Myriam Brugna[1] and Laetitia Shintu[3]*.

[1]Aix Marseille Univ, CNRS, BIP, Marseille, France

[2]MS-Nutrition, Marseille, France

[3]Aix Marseille Univ, CNRS, Centrale Marseille, ISM2, Marseille, France

*Corresponding author: Laetitia Shintu, Institut des Sciences Moléculaires de Marseille, Faculté de Saint Jérôme, av. escadrille Normandie Niémen, 13397 Marseille Cedex 20, France

Email : laetitia.shintu@univ-amu.fr

Phone : +33 413945619

Abstract

Solidesulfovibrio fructosivorans (formely *Desulfovibrio fructosovorans*), an anaerobic sulfate-reducing bacterium, possesses six gene clusters encoding six hydrogenases catalyzing the reversible oxidation of hydrogen gas (H_2) into protons and electrons. One of these, named Hnd, was demonstrated to be an electron-bifurcating hydrogenase Hnd (Kpebe et al., 2018). It couples the exergonic reduction of NAD^+ to the endergonic reduction of a ferredoxin with electrons derived from H_2 and whose function has been recently shown to be involved in ethanol production under pyruvate fermentation (Payne 2022). To understand further the physiological role of Hnd in *S. fructosivorans*, we compared the mutant deleted of part of the *hnd* gene with the wild-type strain grown on pyruvate without sulfate using NMR-based metabolomics. Our results confirm that Hnd is profoundly involved in ethanol metabolism, but also indirectly intervenes in global carbon metabolism and additional metabolic processes such as the biosynthesis of branched-chain amino acids. We also highlight the metabolic reprogramming induced by the deletion of *hndD* that leads to the upregulation of several NADP-dependent pathways.

Highlights

- Metabolomics characterized pathways of pyruvate fermentation in *S. fructosivorans*
- Hnd is involved in ethanol metabolism and branched-chain amino acid biosynthesis.
- HndD deletion leads to the upregulation of NADP-dependent pathways.

Keywords : metabolomics, electron-bifurcating hydrogenase, ethanol metabolism, NADP-dependent pathways, *Desulfovibrio*

Introduction

Desulfovibrio is a genus of sulfate-reducing bacteria that is pervasive in a diverse range of environments. Recently, a new classification of *Desulfovibrio* bacteria has been reported and the genus *Desulfovibrio* has been subdivided into 13 new genera, but in this publication, the term *Desulfovibrio* refers to the genus in the old classification (Waite et al., 2020). *Desulfovibrio* species use sulfate as the terminal electron acceptor for the oxidation of an assortment of electron donors such as lactate, ethanol, formate, and molecular hydrogen (Rabus et al., 2013; Singleton, 1993). Hydrogen in particular plays an important role in the energy metabolism of *Desulfovibrio* species, because not only can hydrogen be used as the sole source of electrons in the presence of a suitable carbon source and electron acceptor, but hydrogen is also released during fermentative growth with certain carbon sources, to regenerate reduced electron carriers (Brandis and Thauer, 1981). Additionally, hydrogen can be consecutively produced and consumed during the degradation of organic compounds during respiration (Odom and Peck, 1981).

Hydrogenases are the critical enzymes implicated in this metabolism, as they catalyze the splitting or synthesis reactions of molecular hydrogen. The number of hydrogenases present varies considerably from one *Desulfovibrio* species to another, but the vast majority of the species are known to contain at least two (Baffert et al., 2019; Pereira et al., 2011). Further hydrogenase diversity in *Desulfovibrio* exists when the type (based on the metal center; [NiFe] or [FeFe]) and the cellular localization (cytoplasm, periplasm or membrane-bound) are considered, and this diversity makes the role of each hydrogenase difficult to determine. An "hydrogen cycling" model for the growth of *Desulfovibrio vulgaris* and *Desulfovibrio gigas* with lactate in the presence of sulfate was proposed (Odom and Peck, 1981). In this model, a cytoplasmic hydrogenase consumes the protons and electrons produced by lactate oxidation in order to produce H_2. The H_2 then diffuses through the cytoplasmic membrane and is re-oxidized by a periplasmic hydrogenase, regenerating the protons and electrons. The produced protons contribute to the proton gradient across the membrane and are used for ATP synthesis. The electrons are captured by the c-type cytochrome network, and they are transferred to various membrane-bound electron-transfer complexes and used for sulfate reduction in the cytoplasm. This model also explains the multiple observations of a rapid and temporal

accumulation of H_2 known as a hydrogen burst when *Desulfovibrio* species are grown on lactate and sulfate (Brandis and Thauer, 1981; Tsuji and Yagi, 1980).

Since the introduction of the hydrogen cycling model forty years ago, others have suggested alternative models that minimize the importance of H_2 evolution on electron transport. Lupton and colleagues presented an alternative hypothesis where H_2 production is not obligatory, but it is used to control the redox state of internal electron carriers. In this model, the organism transports the electrons directly to sulfate through the membrane-bound electron-transfer complexes, and hydrogen evolution occurs only when the rate of electron extraction from an organic donor is greater than the rate at which the electrons are taken up by the sulfate reduction system (Lupton et al., 1984). Following experimental evidence supporting both hypotheses, Noguera and cowokers, and later, Keller and Wall proposed a unified model in which there are two electron transport mechanisms that operate in parallel: one route that is like the hydrogen-cycling model which involves H_2 evolution and another route that does not require H_2 as an intermediate (Keller and Wall, 2011; Noguera et al., 1998). The presence of multiple electron transport mechanisms is thought to promote rapid adaptation of *Desulfovibrio* species to different environments.

In *Solidesulfovibrio fructosivorans* (formely *Desulfovibrio fructosovorans*), our model organism, three hydrogenases have already been characterized biochemically: Hyn, a periplasmic [NiFe] hydrogenase (Hatchikian et al., 1990); Hyd, a periplasmic [FeFe]-type (Casalot et al., 1998) and Hnd, a tetrameric, cytoplasmic [FeFe] hydrogenase (De Luca et al., 1998a, 1998b; Dermoun et al., 2002). In addition to these three, genomic analysis of *S. fructosivorans* revealed genes for three other putative hydrogenases (Baffert et al., 2019): a trimeric, cytoplasmic [FeFe]-type that is structurally similar to the electron-bifurcating hydrogenase Hyd found in *Thermotoga maritima* (Schut and Adams, 2009), a membrane-bound Ech-type (Schoelmerich and Müller, 2020), and a cytoplasmic, [FeFe]-type that has homology with putative phosphatase-linked sensory hydrogenases like Hfs from *Thermoanaerobacter saccharolyticum* (Eminoğlu et al., 2017; Shaw et al., 2009) and HydS from *Ruminococcus albus* (Zheng et al., 2014) or *T. maritima* (Chongdar et al., 2018). Marker-exchange mutagenesis demonstrated an influence of each of these hydrogenases on the growth parameters of the bacterium but failed to establish a specific role for each of

the hydrogenases in the energy metabolism (Casalot et al., 2002; Malki et al., 1997; Rousset et al., 1991), due to a probable compensation mechanism between the different hydrogenases (Casalot et al., 2002).

We recently established that Hnd functions with a flavin-based electron bifurcation mechanism (Kpebe et al., 2018), a method of energy coupling generally found in anaerobic prokaryotes that was first described in 2008 (Li et al., 2008). Hnd couples the reduction of two different electron acceptors: NAD^+, which has a high redox potential and a ferredoxin which has a relatively low redox potential (Kpebe et al., 2018). Reduction of the ferredoxin is thermodynamically unfavorable and would not proceed if the two reactions were not coupled. The "energy rich" reduced ferredoxin can then be used as a source of low potential electrons for other reactions (Buckel and Thauer, 2018; Müller et al., 2018).

Hnd was characterized as an NAD-dependent hydrogenase (Kpebe et al., 2018). Although putative NAD-dependent electron-bifurcating hydrogenases are abundant in anaerobes (Greening et al., 2016), very few have been characterized biochemically and little is known about their metabolic function in vivo. Among the genus *Desulfovibrio*, however, a relatively small number of strains contain genes for putative electron-bifurcating hydrogenases (Baffert et al., 2019; Kpebe et al., 2018). It was recently determined that Hnd plays a key role in the ethanol metabolism of *S. fructosivorans,* as a strain deleted of *hndD* produces only trace amounts of ethanol during pyruvate fermentation compared to the wild-type strain (Payne et al., 2022). Under this condition, we proposed that Hnd oxidizes part of the H_2 produced, probably by Ech, during fermentation generating both NADH and reduced ferredoxin for ethanol production via its electron bifurcation mechanism. Nevertheless, many questions remained about the role of Hnd in the global metabolism of *S. fructosivorans*.

In this context, we decided to explore the function of Hnd in *S. fructosivorans* metabolism using an NMR-based metabolomics approach. Indeed, metabolomics was demonstrated to provide valuable insights regarding the physiological role of specific enzymes in bacteria through comparison between the wild-type and the mutant metabolism (Hubert and de Carvalho, 2022). We report here the extracellular and intracellular metabolic fingerprinting of *S. fructosivorans* wild-type (Ollivier et al., 1988) and SM4 (Δ*hndD*) (Malki et al., 1997) strains grown on pyruvate via liquid state and High Resolution Magic Angle Spinning (HRMAS) NMR-based metabolomics techniques, respectively. Our results demonstrate that the electron

bifurcating reaction catalyzed by Hnd is important for the generation of reducing equivalents (reduced ferredoxin and NADH), which intervene in a variety of metabolic pathways, even those outside the expected processes of carbon metabolism and energy generation.

Material and Methods

Bacterial Strains and Growth Conditions

S. fructosivorans DSM3604 (wild-type strain) (Ollivier et al. 1988) and *S. fructosivorans* SM4 (Δ*hndD*, Cm^R) (Malki et al., 1997) were grown in a culture medium containing 40 mM of pyruvate in absence of sulfate (PS0 medium), as described previously (Payne et al., 2022). Strain SM4 was grown with thiamphenicol 35 $\mu g \cdot mL^{-1}$ (dissolved in methanol) to avoid contamination from other bacteria. Both strains were grown anaerobically at 37 °C in volumes of 100 mL contained in 120 mL glass serum bottles sealed with a butyl rubber stopper and an aluminum crimp top. The medium was inoculated with 5% (v/v) of fresh cultures grown in a pyruvate 40 mM, sulfate 2mM culture medium (PS2 medium) as previously described (Payne et al., 2022). Six biological replicates were inoculated for each strain, with the inoculum originating from the same culture in order to maximize reproducibility. Growth was monitored by OD_{600} measurements. In addition, SM4 strains (n=3) was also grown in a medium exempt of antibiotics following the same protocol to assess the innocuity of the antibiotics on the overall metabolism of the bacteria.

Sample Collection

Samples from each culture were collected after 164 h of culture. To normalize the signals based on the number of cells, the OD_{600} was measured for each culture and a sample of each containing 10^{10} cells was taken (10^{10} cells=10 mL culture @OD_{600}=1). All the following manipulations were performed at 4°C in a cold room. The cells were collected by centrifugation for 5 min at 12,000 g. The supernatant was removed and filtered (0.2 µm pore size cellulose filters) and frozen in liquid N_2 The pellets were washed one time with sterile PBS (137 mM NaCl, 2.7 mM KCl, 1.8 mM KH_2PO_4, 10 mM Na_2HPO_4, pH 7.4), and centrifuged for 5 min at 12,000 g. The pellets were frozen in liquid N_2, and the frozen supernatants and pellets were stored at -80°C until analysis with NMR.

144

145 **^{1}H liquid-state NMR spectroscopy and data processing**

146 Five hundred microliters of each supernatant sample were mixed with 100 µL of D_2O containing 1.68 mM
147 trimethylsilylpropanoic acid (TSP) to act as an internal reference. The samples were then placed into a 5
148 mm NMR tube. Experiments were carried out on a Bruker Avance III spectrometer operating at 600 MHz
149 for the ^{1}H frequency equipped with a TXI probe. A NOESY 1D pulse sequence experiment with a relaxation
150 time of 17.5 s associated with a water presaturation pulse of 2.5 s and an acquisition time of 2.7 s was run
151 on each sample at a temperature of 300 K. The mixing time was set to 10 ms. For each spectrum, 128 free
152 induction decays (FID) of 65K data points were collected using a spectral width of 12,000 Hz. The FIDs
153 were multiplied by an exponential weighting function corresponding to a line broadening of 0.3 Hz and
154 zero-filled once prior to Fourier transformation. ^{1}H NMR spectra were imported into NMRProcFlow v1.4
155 online (Jacob et al., 2017) and divided into buckets using the intelligent bucketing tool with a resolution
156 factor of 0.5 and a signal-to-noise threshold of 1, leading to 345 buckets. The region between 4.50 and 5.20
157 ppm was excluded in order to remove the effect of the water signal presaturation. Signals corresponding to
158 the antibiotic were also removed.

159 **^{1}H HRMAS NMR spectroscopy and data processing**

160 Pellets containing 10^{10} cells were resuspended with 10 µL of D_2O containing 1.68 mM TSP, to
161 provide an internal reference, then added to a 4 mm ZrO_2 HRMAS rotor with a cylindrical insert. All
162 HRMAS experiments were carried out on a Bruker Avance spectrometer operating at 400 MHz for the ^{1}H
163 frequency equipped with a ^{1}H/^{13}C/^{31}P HRMAS probe. Spectra were acquired at 277 K with a spin rate of 4
164 kHz. A Carr−Purcell−Meiboom−Gill (CPMG) NMR spin echo sequence ([presat-90°-(τ-180°-τ)n]) with an
165 overall spin echo time of 25 ms, preceded by a water presaturation pulse during the relaxation delay of 2 s,
166 was used to reduce the signal intensities of lipids and macromolecules. For each spectrum, 256 free
167 induction decays (FID) of 32 k data points were collected using a spectral width of 8000 Hz. The FIDs were
168 multiplied by an exponential weighting function corresponding to a line broadening of 0.5 Hz and zero-
169 filled once prior to Fourier transformation.

^{1}H NMR spectra were manually phased and referenced to the TSP signal (δ = 0 ppm), and automatically baseline corrected and using Topspin 3.5 (Bruker BioSpin GmbH, Karlsruhe, Germany). The spectra were imported into NMRProcFlow v1.4 online (Jacob et al., 2017) and divided into buckets using the intelligent bucketing tool with a resolution factor of 0.5 and a signal-to-noise threshold of 3, leading to 122 buckets. The region between 4.85 and 5.20 ppm was excluded in order to remove the influence of variations in the water presaturation efficiency. The spectral buckets were then normalized to total spectrum intensity using MetaboAnalyst v 3.0.3 (Pang et al., 2020).

Statistical analysis

Statistical analysis was carried out in R v 4.0.3 (R Core Team, 2021) using the mixOmics package (Le Cao et al., 2021). Partial least squares regression (PLS) in canonical mode, an unsupervised statistical method, was performed to relate the intracellular metabolome with the extracellular one. The intra- and extracellular data sets, respectively, the X– and Y- matrices, were integrated and partial least squares regression (PLS) was used to maximize the covariance between both matrix variables. With this analysis, latent variables, linear combinations of the NMR variables from both blocks were calculated, so that NMR variables sharing the same pattern participate equally in the discrimination between the samples.

Metabolite quantification

Relevant metabolites from the culture supernatant samples were quantified using Chenomx NMR Suite 9.0 software (Chenomx, Inc; Edmonton, AB, CA). Using the Processor tool, the spectra were calibrated using the internal standard of 0.28 mM TSP as the reference. The reference metabolite spectra were then fitted to the sample spectra using the Profiler tool. The absolute concentration values were then normalized according to the OD600 for each sample, i.e. according to the final number of cells in each bottle.

Concerning the quantification of the intracellular metabolites, the TSP signal cannot be used directly for quantification since TSP binds to proteins and other macromolecules, which affects the intensity of its signal. The ERETIC method, calibrated on a sample of 1.06 mM 2-oxoglutarate, was thus used to quantify the free-TSP signal (Akoka et al., 1999). Metabolites were then quantified using Chenomx NMR suite 9.0 as explained previously. For each quantified metabolite, two-tailed Student t-test was used to calculate the p-value of the discrimination between WT and SM4 samples. The fermentation balance was calculated as

the ratio between the produced metabolite concentration and the consumed pyruvate concentration. It is expressed in mol/mol pyruvate.

Data availability

Acquired NMR spectra can be found in the following Mendeley dataset: https://doi.org/10.17632/t99vf4w5tf.1

Results

Identification of intra- and extracellular metabolites under pyruvate fermentation using NMR spectroscopy

WT and *hndD* deletion mutant (SM4) strains were grown in a sulfate-free medium containing pyruvate as the sole source of carbon (PS0 medium). As presented on Figure S1, the growth rates were 0.006 h^{-1} and 0.005 h^{-1} for WT and SM4 strains, respectively. Pyruvate was consumed at a rate of 0.62 +/- 0.01 mM/h for both strains. Hnd does not appear to be crucial for *S. fructosivorans* growth, as both strains reach similar final OD_{600} values (Figure S1). The ^{1}H NMR spectra of the spent culture media from WT (n=3), SM4 grown with antibiotics (n=3) and SM4 without antibiotics (n=3) samples was also recorded and analyzed using principal component analysis (PCA). The PC2 vs PC3 score plot, presented in Figure S2, shows a clear clustering of all SM4 samples without discrimination between the ones exposed to the antibiotics and the others. This validates the innocuity of the antibiotics on the overall metabolism of the SM4 strains.

To better understand the physiological role of Hnd during fermentative H_2-production, the metabolism of wild type strain was compared with the one of the SM4 mutant strain for which *hndD* encoding the catalytic subunit of the Hnd hydrogenase was deleted. The modulations of the global bacterial metabolism, i.e. extracellular (culture medium) and intracellular metabolites (bacterium cells), were analyzed using NMR-based metabolomics.

The extracellular and intracellular metabolic ^{1}H NMR profiles of the WT and SM4 samples were recorded using liquid-state and HRMAS NMR spectroscopy, respectively. Representative spectra of extracellular and intracellular metabolites for both strains are presented in Figure 1 and S3, respectively.

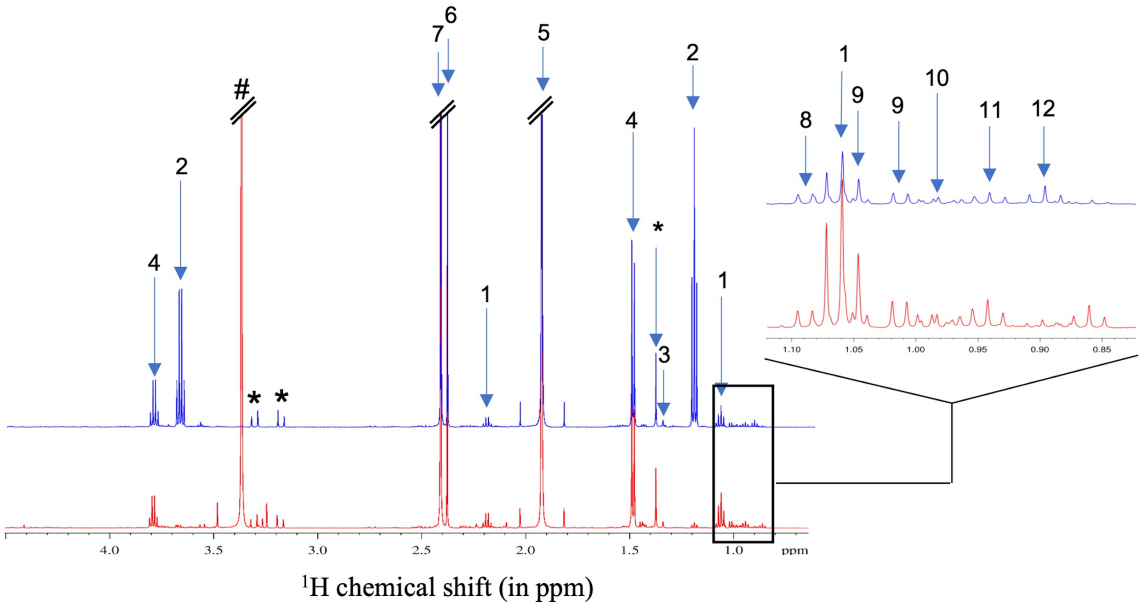

Fig. 1 Representative ^{1}H NMR spectra of *S. fructosivorans* WT (blue) and SM4 (red) PS0 spent culture medium (after 164 h growth). * = pyruvate dimer signals; # = methanol from antibiotic. Assignments: 1: propionate; 2: ethanol; 3: lactate; 4: alanine; 5: acetate; 6: pyruvate; 7: succinate; 8: methylsuccinate; 9: valine; 10: 2-aminobutyrate; 11: isoleucine; 12: 3-methyl-2-oxovalerate. Only major metabolites are represented on the figure. Assignments of all identified metabolites are reported in Table S1.

The assignments of all the identified metabolites (intra- and extracellular compounds) are reported in Table S1. The intracellular NMR profile of the *S. fructosivorans* WT strain was dominated by the signals of trehalose, alanine, lysine, ethanol, succinate, acetate and an intense unknown signal at 3.72 ppm. Less concentrated metabolites such as NAD(P)$^+$, adenosine monophosphate, glutamate, 2-hydroxyisobutyrate and inosine were also identified. Some metabolites, mainly amino acids, short chain fatty acids and their derivatives and other organic acids were also identified in the spent culture medium.

Metabolic profiling of *S. fructosivorans* under pyruvate fermentation conditions

To identify the metabolites discriminating between WT and SM4 samples, unsupervised canonical PLS analysis was then performed using intracellular and extracellular NMR data as X- and Y-matrices, respectively. The resulting score plot displayed a clear discrimination between both strains and discriminant

extracellular and intracellular metabolites are presented on the loading plot (Figure 2A and 2B). Since the PLS analysis is an unsupervised method, no validation of the model robustness was necessary.

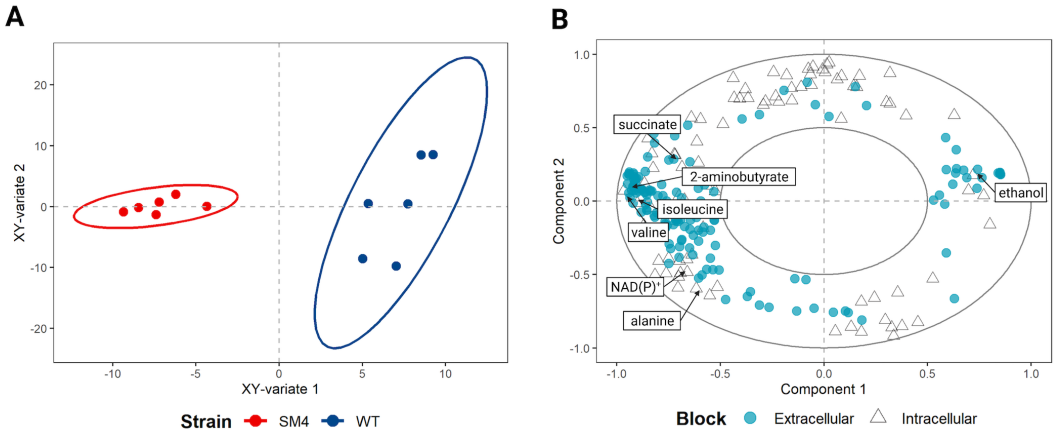

Fig. 2 PLS score (a) and loadings (b) plots performed on ^{1}H NMR spectra of PS0 WT and SM4 samples. Each point on the score plot represents an individual sample. Each point on the loadings plot represents a spectral bucket. The most discriminant metabolites are mentioned on the loading plot.

The loss of Hnd in *S. fructosivorans* led to the accumulation of intracellular NAD(P)$^{+}$, AMP, alanine and valine in the mutant strain compared to the WT strain. Quantification of these four significant metabolites were performed using the ERETIC method (Fig. 3). NAD(P)$^{+}$ and AMP levels were 3 times higher in the mutant than in the WT strain when alanine and valine levels were increased by 2-fold (Table S2).

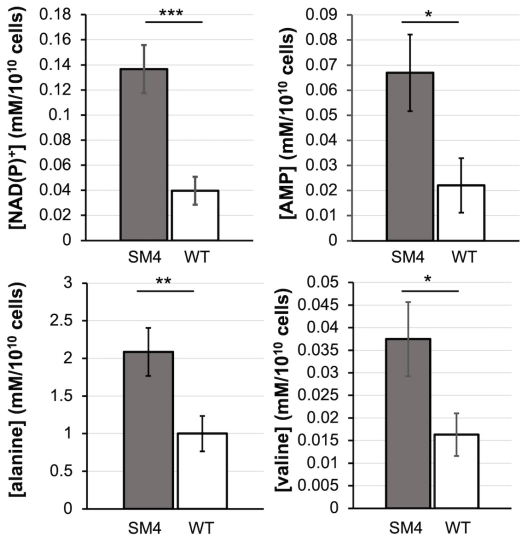

255

256 **Fig. 3** Absolute concentrations (in mM) of the intracellular discriminant metabolites between *S. fructosivorans* WT
257 and SM4 mutant strains grown under pyruvate fermentation conditions. Normalization was not necessary since the
258 number of cells is identical for each sample. ***: p-value <0.001, **: p-value <0.01; *: p-value <0.05

259

260 The PLS results indicated also that the deletion of *hnd* affected the levels of the excreted metabolites (Fig.
261 4).

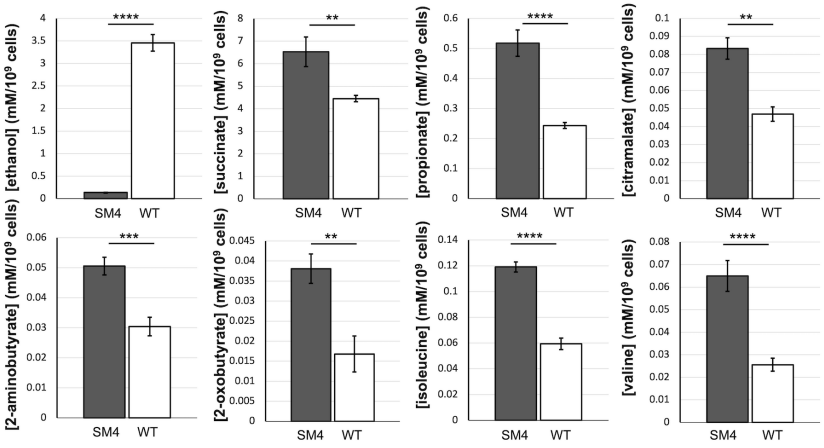

262

263 **Fig. 4** Absolute concentrations (in mM) of the extracellular discriminant metabolites between *S. fructosivorans* WT
264 and SM4 mutant strains grown under pyruvate fermentation. Concentrations were normalized according to the number
265 of cells at the time of collection. ****: p-value <0.0001, ***: p-value <0.001; **: p-value <0.01

266

267 The levels of propionate, 2-aminobutyrate, 2-oxobutyrate, citramalate, valine, isoleucine, and succinate
268 were higher in the mutant while, as expected, the level of excreted ethanol was dramatically reduced. The

fold changes and p-values for each quantified metabolite are reported in Table S3. The quantification of these metabolites showed that pyruvate was mainly fermented into acetate, ethanol and succinate. To clarify the stoichiometry of pyruvate fermentation into these metabolites, we calculated the fermentation balance, i.e. the amount of produced metabolites in mole *per* mole of fermented pyruvate, which is reported in table 1.

Table 1. Fermentation balance for the major products of pyruvate fermentation

Strains	Acetate (mol/mol pyruvate)	Ethanol (mol/mol pyruvate)	Succinate (mol/mol pyruvate)
WT	0.77	0.09	0.12
SM4	0.79	0.004	0.18

The fermentation balance shows that the discrepancy of ethanol production in the SM4 strain led to a diversion of the metabolic fluxes towards mainly the production of succinate, and towards the production of acetate to a lesser extent.

Discussion

Our group previously demonstrated that Hnd is involved in ethanol production during pyruvate fermentation (Payne et al., 2022). However, this involvement is non-essential, as the growth rate and the rate of pyruvate consumption remained similar for both strains. This raised further questions about other pathways in which Hnd could potentially be involved. To further clarify the role of Hnd in *S. fructosivorans* metabolism, a metabolomics approach was carried out on WT and SM4 strains.

To elucidate the secondary pathways influenced by Hnd, we characterized first the metabolism of *S. fructosivorans* WT strain during pyruvate fermentation using NMR spectroscopy. One of the major intracellular metabolites identified was α,α-trehalose, a disaccharide consisting of two glucose monomers. Several *Desulfovibrio* species have been shown to synthesize polyglucose molecules which serve as a storage polymer, and the conditions inducing polyglucose accumulation vary between species (Fareleira et al., 1997; Santos et al., 1993; Stams et al., 1983; Van Niel and Gottschal, 1998). For example, in *D. vulgaris* str. Hildenborough, polyglucose accumulation is caused by limiting Fe^{2+} and NH_4^+ in the growth medium,

whereas in *D. gigas,* high levels of polyglucose are accumulated regardless of the growth condition (Stams et al., 1983). In *D. gigas* (now *Megalodesulfovibrio gigas*), the degradation of polyglucose has been shown to provide reducing potential to produce nucleoside triphosphates under both fermentative and respiratory conditions, and to aid in survival after exposure to O_2 (Fareleira et al., 1997). Trehalose specifically was accumulated in *D. halophilus* (now *Pseudodesulfovibrio halophilus*) in response to increasing medium osmolarity (Welsh et al., 1996). However, in our study, α,α-trehalose content was not affected by the deletion of *hndD* suggesting that it may not be involved in the pyruvate fermentation process. This was also demonstrated by van Niel et al. in *D. salexigens* Mast1 (now *Maridesulfovibrio salexigens*) for which very little polyglucose was accumulated during pyruvate fermentation (Van Niel et al., 1996).

The other major identified intracellular metabolites were the markers of pyruvate fermentation, such as acetate, succinate, and ethanol. These metabolites were also detected in high concentration in the spent culture medium, which would imply that they are first accumulated in the cells before being excreted in the medium. Other end-products of the pyruvate fermentation, such as lactate, propanoate, formate, butyrate, and butanol, could only be detected in the spent culture medium, meaning that these are transient intracellular metabolites.

In addition, we identified intracellular amino acids such as alanine, isoleucine, valine, glutamate, and lysine, which were all detected in the spent culture medium as well, except for glutamate and lysine. Furthermore, the examination of the spent culture medium enabled us to identify other metabolites such as citramalate, 2-oxobutyrate and 3-methyl-2-oxovalerate. Except for lysine, all these metabolites belong to interconnected biosynthesis pathways in which pyruvate plays a central role (Fig. 5).

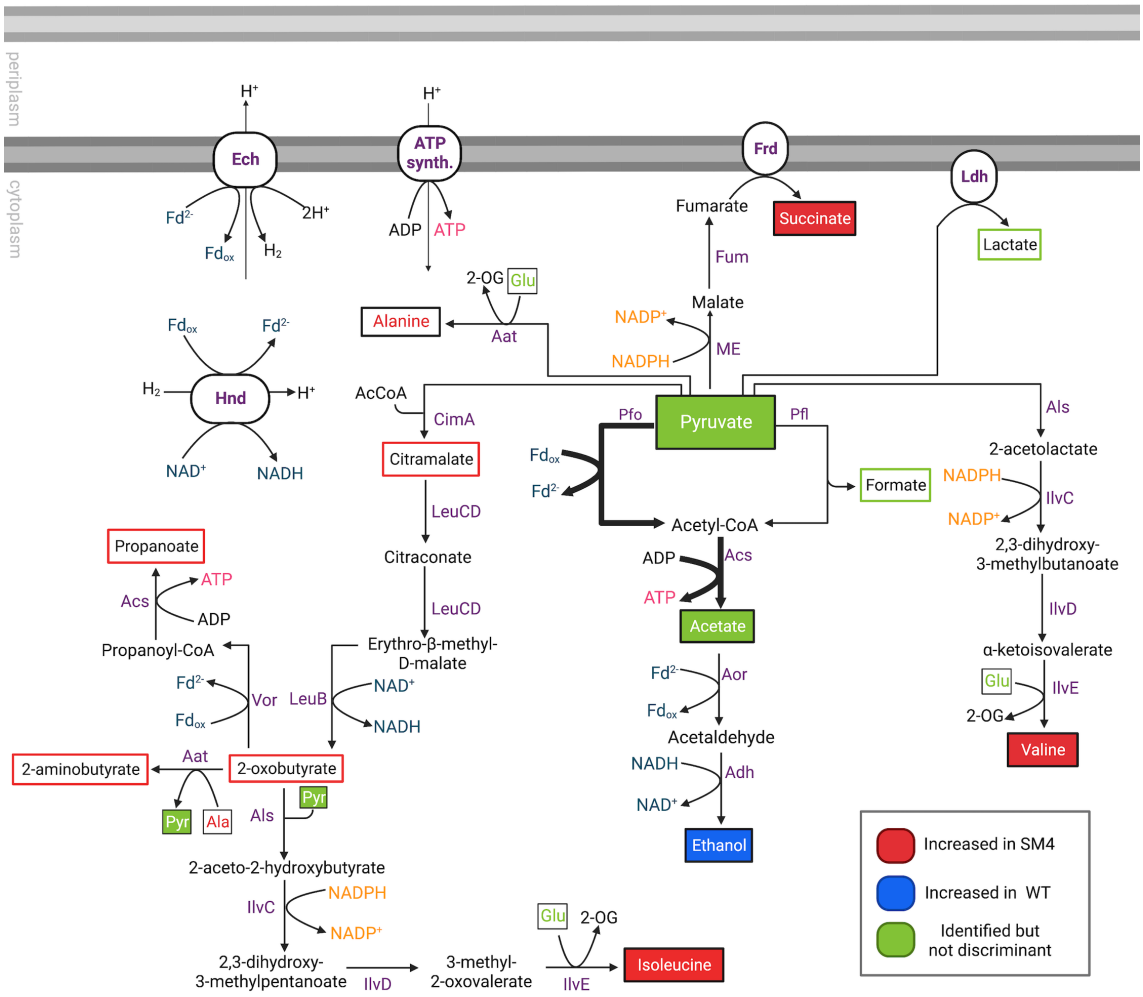

Fig.5 *S. fructosivorans* metabolic pathways active during pyruvate fermentation. One of the major produced metabolite is acetate formed from the one-step conversion of acetyl-CoA through acetyl-CoA synthase (Vita et al., 2015). In the WT strain, ethanol is formed as a minor fermentation product with acetate and acetaldehyde as intermediary metabolites. When *hnd* is deleted, in strain SM4, ethanol is not formed, and flux is redirected to form higher concentrations of succinate and the branched-chain amino acids isoleucine and valine. 2-oxobutyrate, a cytotoxic intermediate in L-isoleucine biosynthesis, is metabolized into 2-aminobutyrate and propanoate. All detected metabolites are framed. Colored letters framed in black indicates the metabolite is exclusively intracellular; black letters framed in color indicates the metabolite is exclusively extracellular; white letters with a filled frame in color indicates the metabolite is both intra- and extracellular. The color indicates in which strain the metabolite concentration is increased: red = increased in SM4; blue = increased in WT; green = metabolite was identified but not discriminant. Bold arrows indicate the pathways with increased flux in SM4. The names of the enzymes catalyzing each reaction are indicated in purple. Aat: alanine aminotransferase; Acs: acetyl-CoA synthase; Adh: alcohol dehydrogenase; Als: acetolactate synthase; Aor: aldehyde ferredoxin oxidoreductase; Cim: citramalate synthase; Ech: energy-converting

hydrogenase; Frd: fumarate reductase; Fum: fumarase; Hnd: tetrameric electron-bifurcating hydrogenase; IlvC: ketol-acid reductoisomerase; IlvD: dihydroxy-acid dehydratase; IlvE: branched-chain amino acid aminotransferase; Kor: ketoisovalerate oxidoreductase; Ldh: lactate dehydrogenase; LeuB: 3-isopropylmalate dehydrogenase; LeuCD: 3-isopropylmalate dehydratase/isomerase; ME: NADP-malic enzyme; Pfl: pyruvate formate-lyase; Por: pyruvate ferredoxin oxidoreductase. AcCoA: acetyl-CoA; Ala: alanine; Fd: ferredoxin; Glu: glutamate; 2-OG: 2-oxoglutarate

Pyruvate reacts with glutamate and is converted into L-alanine and 2-oxoglutarate through the action of an alanine aminotransferase. L-valine is also synthesized from pyruvate, with the NADPH-dependent ketol-acid reductoisomerase acting in an intermediate step. Interestingly, the presence of citramalate, 2-oxobutyrate, and 3-methyl-2-oxovalerate suggests that in *S. fructosivorans*, isoleucine is formed from an alternative biosynthesis pathway from pyruvate and acetyl-CoA instead of threonine. This pathway was introduced as the primary pathway to produce isoleucine in *Geobacter sulfurreducens* (Risso et al., 2008), but has never been previously described for *Desulfovibrio*. The intermediate 2-oxobutyrate was further metabolized directly to 2-aminobutyrate by the alanine aminotransferase or to propanoate with propanoyl-CoA as the intermediary metabolite.

The primary effect of the deletion of *hnd* was the difference in ethanol content in the mutant strain. This is concurrent with the results previously presented demonstrating that Hnd was involved in the process of ethanol formation from pyruvate in the absence of sulfate (Payne et al., 2022). We showed decreased levels of gene expression for two enzymes, aldehyde:ferredoxin oxidoreductase (Aor) and alcohol dehydrogenase (Adh) in strain SM4, enzymes which are responsible for the conversion of acetate into acetaldehyde, then into ethanol. Our metabolomics analysis confirmed that, in absence of Hnd, the fermentation process of pyruvate was interrupted before the formation of ethanol. Considering the increased concentration of succinate produced in strain SM4, the pyruvate that is not metabolized into ethanol appears to be redirected to the pathway of succinate formation via malate and fumarate, which is confirmed by the fermentation balance presented in table 1. The oxidation of pyruvate to malate in *Desulfovibrio* is catalyzed by the NADP-dependent malic enzyme (Kremer et al., 1989), which was shown to be critical for growth during pyruvate fermentation in *D. alaskensis* G20 (now *Oleidesulfovibrio alaskensis*) (Meyer et al., 2014). The reduction of fumarate to succinate is catalyzed by the membrane-bound fumarate reductase complex FrdABC, which

reduces succinate with electrons derived from the menaquinol pool (Meyer et al., 2014; Thauer et al., 2007). Both enzymes catalyze reactions that are independent of NAD and ferredoxin, thus not linked to Hnd via these redox partners. In some organisms, succinate efflux is coupled to the generation of an ion gradient, but in *S. fructosivorans*, it is still unclear what transporter is involved in succinate excretion. No homologs of known anaerobic C4-dicarboxylic acid transporters (Dcu family) (Engel et al., 1994; Kleefeld et al., 2009; Zientz et al., 1996) were found in the genome of *D. fructosivorans*, nor were homologs of the TRAP transporters (Tripartite ATP-independent periplasmic transporters) (Rosa et al., 2018) as was reported in *O. alaskensis* G20 (Meyer et al., 2014). The most likely candidates are two proteins with CitT-like domains (DesfrDRAFT_1398 and 1718), but in *Escherichia coli* CitT is predicted to function as a citrate/succinate antiporter and is utilized when cells ferment citrate (Pos et al., 1998). In *O. alaskensis,* the efflux of succinate was linked to the generation of a chemiosmotic gradient due to the symport of protons (Meyer et al., 2014), but with the lack of a known succinate transporter homolog in *S. fructosivorans*, this conclusion cannot be drawn.

We also observed increased production of the branched-chain amino acids, valine and isoleucine, in strain SM4. The ketol-acid reductoisomerase IlvC is involved in the biosynthesis of both valine and isoleucine and is dependent on NADPH (Rane and Calvo, 1997), as is the malic enzyme. It is therefore plausible that pyruvate oxidation in strain SM4 is redirected to pathways that are dependent on NADPH, away from the ethanol production pathway which is dependent on NADH and therefore correlated to the presence of Hnd. 2-oxobutyrate is a central metabolite formed in the isoleucine biosynthesis pathway, but due to its cytotoxicity (Fang et al., 2021), it is exported from the cell or metabolized to propanoate or 2-aminobutyrate. An increased concentration of intracellular alanine was also observed in strain SM4. The amino group from alanine is transferred by the alanine aminotransferase to 2-oxobutyrate to form 2-aminobutyrate, thus the increased production of alanine in SM4 could correspond with the increased production of 2-aminobutyrate. The diversion of pyruvate oxidation from ethanol production to pathways dependent on NADPH is a likely compensation mechanism due to the loss of a source of NADH when *hndD* is deleted. However, increased amounts of NADPH are needed in SM4 compared to the WT in order to sustain the flux through these pathways. A potential source of NADPH is the putative electron-bifurcating hydrogenase Hnt

(DesfrDRAFT_0985-0987), identified by our team (Baffert et al., 2019). This trimeric enzyme is encoded in the same cluster as genes encoding for the malic enzyme, fumarase and fumarate reductase, which gives an indication of its function in malate and fumarate metabolism. However, no biochemical or genetic studies have been carried out on Hnt, and further works have to be performed to understand better its physiological function. It does, however, seem rational that *S. fructosivorans* would have two different bifurcating hydrogenases with specificities for different redox cofactors. In this case, Hnt would be consuming H_2 and producing reduced ferredoxin and NADPH, albeit at a slower rate than Hnd, because strain SM4 produces more H_2 compared to the WT (Payne et al., 2022).

Metabolomics analysis of *S. fructosivorans* WT and SM4 (*ΔhndD*) was able to confirm that Hnd was mainly involved in the pathway of ethanol production under pyruvate fermentation, which was dramatically downregulated in the SM4 strain. We also highlighted the metabolic reprogramming that took place in which several NADP-dependent pathways, including succinate production and branched-chain amino acid biosynthesis, were upregulated due to the deletion of *hndD*.

Acknowledgements

Our work is supported by CNRS and Aix-Marseille Université. This project has received funding from the European Union's Horizon 2020 research and innovation programme under the Marie Skłodowska-Curie grant agreement No713750. It has also been carried out with the financial support of the Regional Council of Provence-Alpes-Côte d'Azur and with the financial support of the A*MIDEX (n° ANR- 11-IDEX-0001-02), funded by the Investissements d'Avenir project funded by the French Government, managed by the French National Research Agency (ANR).

Declaration of interest

The authors have no conflict of interest to declare.

Author statement

MB and LS conceptualized and designed the study. NP, AK, CG, CB, MB performed the microbiological experiments and cell culture. NP performed the metabolomic analysis. MM, TH, FT, MB and LS supervised the study. NP, MB and LS interpreted the results. NP and LS drafted the manuscript. All co-authors

participated in the critical review of the final manuscript. All authors have read and approved the revised version of the manuscript.

References

Akoka, S., Barantin, L., Trierweiler, M., 1999. Concentration Measurement by Proton NMR Using the ERETIC Method. Anal. Chem. 71, 2554–2557. https://doi.org/10.1021/AC981422I

Baffert, C., Kpebe, A., Avilan, L., Brugna, M., 2019. Hydrogenases and H 2 metabolism in sulfate-reducing bacteria of the Desulfovibrio genus. Adv. Microb. Physiol. https://doi.org/10.1016/bs.ampbs.2019.03.001

Brandis, A., Thauer, R.K., 1981. Growth of Desulfovibrio species on hydrogen and sulphate as sole energy source. J. Gen. Microbiol. 126, 249–252. https://doi.org/10.1099/00221287-126-1-249

Buckel, W., Thauer, R.K., 2018. Flavin-based electron bifurcation, ferredoxin, flavodoxin, and anaerobic respiration with protons (Ech) or NAD+ (Rnf) as electron acceptors: A historical review. Front. Microbiol. 9. https://doi.org/10.3389/fmicb.2018.00401

Casalot, L., Hatchikian, C.E., Forget, N., De Philip, P., Dermoun, Z., Bélaïch, J.P., Rousset, M., 1998. Molecular study and partial characterization of iron-only hydrogenase in Desulfovibrio fructosovorans. Anaerobe 4, 45–55. https://doi.org/10.1006/anae.1997.0137

Casalot, L., Valette, O., De Luca, G., Dermoun, Z., Rousset, M., De Philip, P., 2002. Construction and physiological studies of hydrogenase depleted mutants of Desulfovibrio fructosovorans. FEMS Microbiol. Lett. 214, 107–112. https://doi.org/10.1016/S0378-1097(02)00852-2

Chongdar, N., Birrell, J.A., Pawlak, K., Sommer, C., Reijerse, E.J., Rüdiger, O., Lubitz, W., Ogata, H., 2018. Unique Spectroscopic Properties of the H-Cluster in a Putative Sensory [FeFe] Hydrogenase. J. Am. Chem. Soc. 140, 1057–1068. https://doi.org/10.1021/jacs.7b11287

De Luca, G., Asso, M., Bélaïch, J.P., Dermoun, Z., 1998a. Purification and characterization of the HndA subunit of NADP-reducing hydrogenase from Desulfovibrio fructosovorans overproduced in Escherichia coli. Biochemistry 37, 2660–2665. https://doi.org/10.1021/bi972474p

De Luca, G., De Philip, P., Rousset, M., Belaich, J.-P., Dermoun, Z., 1998b. The NADP-Reducing hydrogenase of Desulfovibrio fructosovorans: Evidence for a native complex with hydrogen-dependent methyl-viologen-reducing activity. Biochem. Biophys. Res. Commun. 248, 591–596. https://doi.org/10.1006/bbrc.1998.9022

Dermoun, Z., De Luca, G., Asso, M., Bertrand, P., Guerlesquin, F., Guigliarelli, B., 2002. The NADP-reducing hydrogenase from Desulfovibrio fructosovorans: Functional interaction between the C-terminal region of HndA and the N-terminal region of HndD subunits. Biochim. Biophys. Acta - Bioenerg. 1556, 217–225. https://doi.org/10.1016/S0005-2728(02)00364-X

Eminoğlu, A., Murphy, S.J.L., Maloney, M., Lanahan, A., Giannone, R.J., Hettich, R.L., Tripathi, S.A., Beldüz, A.O., Lynd, L.R., Olson, D.G., 2017. Deletion of the hfsB gene increases ethanol production

in Thermoanaerobacterium saccharolyticum and several other thermophilic anaerobic bacteria. Biotechnol. Biofuels 10, 1–11. https://doi.org/10.1186/s13068-017-0968-9

Engel, P., Kramer, R., Unden, G., 1994. Transport of C4-dicarboxylates by anaerobically grown Escherichia coli. Energetics and mechanism of exchange, uptake and efflux. Eur. J. Biochem. 222, 605–614. https://doi.org/10.1111/J.1432-1033.1994.TB18903.X

Fang, Y., Zhang, S., Wang, J., Yin, L., Zhang, H., Wang, Z., Song, J., Hu, X., Wang, X., 2021. Metabolic detoxification of 2-oxobutyrate by remodeling Escherichia coli acetate bypass. Metabolites 11, 1–17. https://doi.org/10.3390/metabo11010030

Fareleira, P., Legall, J., Xavier, A.V., Santos, H., 1997. Pathways for utilization of carbon reserves in Desulfovibrio gigas under fermentative and respiratory conditions. J. Bacteriol. 179, 3972–3980. https://doi.org/10.1128/jb.179.12.3972-3980.1997

Greening, C., Biswas, A., Carere, C.R., Jackson, C.J., Taylor, M.C., Stott, M.B., Cook, G.M., Morales, S.E., 2016. Genomic and metagenomic surveys of hydrogenase distribution indicate H 2 is a widely utilised energy source for microbial growth and survival. ISME J. 10, 761–777. https://doi.org/10.1038/ismej.2015.153

Hatchikian, E.C., Traore, A.S., Fernandez, V.M., Cammack, R., 1990. Characterization of the nickel-iron periplasmic hydrogenase from Desulfovibrio fructosovorans. Eur. J. Biochem. 187, 635–643. https://doi.org/10.1111/J.1432-1033.1990.TB15347.X

Hubert, C.B., de Carvalho, L.P.S., 2022. Metabolomic approaches for enzyme function and pathway discovery in bacteria, in: Methods in Enzymology. Elsevier, pp. 29–47. https://doi.org/10.1016/bs.mie.2021.12.001

Jacob, D., Deborde, C., Lefebvre, M., Maucourt, M., Moing, A., 2017. NMRProcFlow: a graphical and interactive tool dedicated to 1D spectra processing for NMR-based metabolomics. Metabolomics 13, 1–5. https://doi.org/10.1007/s11306-017-1178-y

Keller, K.L., Wall, J.D., 2011. Genetics and molecular biology of the electron flow for sulfate respiration in Desulfovibrio. Front. Microbiol. 2, 1–17. https://doi.org/10.3389/fmicb.2011.00135

Kleefeld, A., Ackermann, B., Bauer, J., Krämer, J., Unden, G., 2009. The fumarate/succinate antiporter DcuB of escherichia Coli is a bifunctional protein with sites for regulation of DcuS-dependent gene expression. J. Biol. Chem. 284, 265–275. https://doi.org/10.1074/ 10.1074/jbc.M807856200

Kpebe, A., Benvenuti, M., Guendon, C., Rebai, A., Fernandez, V., Le Laz, S., Etienne, E., Guigliarelli, B., García-Molina, G., de Lacey, A.L., Baffert, C., Brugna, M., 2018. A new mechanistic model for an O2-protected electron-bifurcating hydrogenase, Hnd from Desulfovibrio fructosovorans. Biochim. Biophys. Acta - Bioenerg. 1859, 1302–1312. https://doi.org/10.1016/j.bbabio.2018.09.364

Kremer, D.R., Timmer, C.J., Hansen, T.A., 1989. Catabolism of malate and related dicarboxylic acids in various Desulfovibrio strains and the involvement of an oxygen-labile NADPH dehydrogenase. Arch. Microbiol. 151, 34–39.

Le Cao, K.-A., Rohart, F., Gonzalez, I., Dejean, S., Gautier, B., Bartolo, F., Monget, P., Coquery, J., Yao, F., Liquet, B., 2021. mixOmics.

Li, F., Hinderberger, J., Seedorf, H., Zhang, J., Buckel, W., Thauer, R.K., 2008. Coupled Ferredoxin and Crotonyl Coenzyme A (CoA) Reduction with NADH Catalyzed by the Butyryl-CoA Dehydrogenase / Etf Complex from Clostridium kluyveri. J. Bacteriol. 190, 843–850. https://doi.org/10.1128/JB.01417-07

Lupton, F.S., Conrad, R., Zeikus, J.G., 1984. Physiological function of hydrogen metabolism during growth of sulfidogenic bacteria on organic substrates. J. Bacteriol. 159, 843–849. https://doi.org/10.1128/jb.159.3.843-849.1984

Malki, S., De Luca, G., Fardeau, M.L., Rousset, M., Belaich, J.P., Dermoun, Z., 1997. Physiological characteristics and growth behavior of single and double hydrogenase mutants of Desulfovibrio fructosovorans. Arch. Microbiol. 167, 38–45. https://doi.org/10.1007/s002030050414

Meyer, B., Kuehl, J.V., Price, M.N., Ray, J., Deutschbauer, A.M., Arkin, A.P., Stahl, D.A., 2014. The energy-conserving electron transfer system used by Desulfovibrio alaskensis strain G20 during pyruvate fermentation involves reduction of endogenously formed fumarate and cytoplasmic and membrane-bound complexes, Hdr-Flox and Rnf. Environ. Microbiol. 16, 3463–3486. https://doi.org/10.1111/1462-2920.12405

Müller, V., Chowdhury, N.P., Basen, M., 2018. Electron Bifurcation: A Long-Hidden Energy-Coupling Mechanism. Annu. Rev. Microbiol. 72, 331–353. https://doi.org/10.1146/annurev-micro-090816-093440

Noguera, D.R., Brusseau, G.A., Rittmann, B.E., Stahl, D.A., 1998. A unified model describing the role of hydrogen in the growth of Desulfovibrio vulgaris under different environmental conditions. Biotechnol. Bioeng. 59, 732–746. https://doi.org/10.1002/(SICI)1097-0290(19980920)59:6<732::AID-BIT10>3.0.CO;2-7

Odom, J.M., Peck, H.D., 1981. Hydrogen cycling as a general mechanism for energy coupling in the sulfate-reducing bacteria, Desulfovibrio sp. FEMS Microbiol. Lett. 12, 47–50. https://doi.org/10.1111/j.1574-6968.1981.tb07609.x

Ollivier, B., Cord-Ruwisch, R., Hatchikian, E.C., Garcia, J.L., 1988. Characterization of Desulfovibrio fructosovorans sp. nov. Arch. Microbiol. 149, 447–450. https://doi.org/10.1007/BF00425586

Pang, Z., Chong, J., Li, S., Xia, J., 2020. MetaboAnalystR 3.0: Toward an Optimized Workflow for Global Metabolomics. Metab. 2020 Vol 10 Page 186 10, 186. https://doi.org/10.3390/METABO10050186

Payne, N., Kpebe, A., Guendon, C., Baffert, C., Ros, J., Lebrun, R., Denis, Y., Shintu, L., Brugna, M., 2022. The electron-bifurcating FeFe-hydrogenase Hnd is involved in ethanol metabolism in Desulfovibrio fructosovorans grown on pyruvate. Mol. Microbiol. https://doi.org/10.1111/MMI.14881

Pereira, I.A.C., Ramos, A.R., Grein, F., Marques, M.C., da Silva, S.M., Venceslau, S.S., 2011. A comparative genomic analysis of energy metabolism in sulfate reducing bacteria and archaea. Front.

Microbiol. 2, 1–22. https://doi.org/10.3389/fmicb.2011.00069

Pos, K.M., Dimroth, P., Bott, M., 1998. The Escherichia coli citrate carrier CitT: a member of a novel eubacterial transporter family related to the 2-oxoglutarate/malate translocator from spinach chloroplasts. J. Bacteriol. 180, 4160–4165. https://doi.org/10.1128/JB.180.16.4160-4165.1998

R Core Team, 2021. R: A language and environment for statistical computing.

Rabus, R., Hansen, T.A., Widdel, F., 2013. Dissimilatory Sulfate- and Sulfur-Reducing Prokaryotes, in: Rosenberg, E., DeLong, E.F., Lory, S., Stackebrandt, E., Thompson, F. (Eds.), The Prokaryotes. Springer-Verlag, pp. 309–404. https://doi.org/10.1007/0-387-30742-7_15

Rane, M.J., Calvo, K.C., 1997. Reversal of the nucleotide specificity of ketol acid reductoisomerase by site-directed mutagenesis identifies the NADPH binding site. Arch. Biochem. Biophys. 338, 83–89. https://doi.org/10.1006/abbi.1996.9802

Risso, C., Van Dien, S.J., Orloff, A., Lovley, D.R., Coppi, M.V., 2008. Elucidation of an alternate isoleucine biosynthesis pathway in Geobacter sulfurreducens. J. Bacteriol. 190, 2266–2274. https://doi.org/10.1128/JB.01841-07

Rosa, L.T., Bianconi, M.E., Thomas, G.H., Kelly, D.J., 2018. Tripartite ATP-independent periplasmic (TRAP) transporters and Tripartite Tricarboxylate Transporters (TTT): From uptake to pathogenicity. Front. Cell. Infect. Microbiol. 8, 33. https://doi.org/10.3389/FCIMB.2018.00033/BIBTEX

Rousset, M., Dermoun, Z., Chippaux, M., Bélaich, J.P., 1991. Marker exchange mutagenesis of the hydN genes in Desulfovibrio fructosovorans. Mol. Microbiol. 5, 1735–1740. https://doi.org/10.1111/j.1365-2958.1991.tb01922.x

Santos, H., Fareleira, P., Xavier, A.V., Chen, L., Liu, M.-Y., Le Gall, J., 1993. Aerobic metabolism of carbon reserves by the “obligate anaerobe” Desulfovibrio gigas. Biochem. Biophys. Res. Commun. 195, 551–557.

Schoelmerich, M.C., Müller, V., 2020. Energy-converting hydrogenases: the link between H2 metabolism and energy conservation. Cell. Mol. Life Sci. 77, 1461–1481. https://doi.org/10.1007/s00018-019-03329-5

Schut, G.J., Adams, M.W.W., 2009. The iron-hydrogenase of Thermotoga maritima utilizes ferredoxin and NADH synergistically: A new perspective on anaerobic hydrogen production. J. Bacteriol. 191, 4451–4457. https://doi.org/10.1128/JB.01582-08

Shaw, A.J., Hogsett, D.A., Lynd, L.R., 2009. Identification of the [FeFe]-hydrogenase responsible for hydrogen generation in Thermoanaerobacterium saccharolyticum and demonstration of increased ethanol yield via hydrogenase knockout. J. Bacteriol. 191, 6457–6464. https://doi.org/10.1128/JB.00497-09

Singleton, R., 1993. The sulfate reducing bacteria: an overview, in: Singleton, R., Odom, J.M. (Eds.), The Sulfate-Reducing Bacteria: Contemporary Perspectives. Springer-Verlag, pp. 1–20.

Stams, F.J.M., Veenhuis, M., Weenk, G.H., Hansen, T.A., 1983. Occurrence of polyglucose as a storage

polymer in Desulfovibrio species and Desulfobulbus propionicus. Arch. Microbiol. 330, 54–59.

Thauer, R.K., Stackebrandt, E., Hamilton, W.A., 2007. Energy metabolism and phylogenetic diversity of sulphate-reducing bacteria, in: Barton, L.L., Hamilton, W.A. (Eds.), Sulphate-Reducing Bacteria: Enviromental and Engineered Systems. Cambridge University Press, pp. 1–38.

Tsuji, K., Yagi, T., 1980. Significance of hydrogen burst from growing cultures of Desulfovibrio vulgaris, Miyazaki, and the role of hydrogenase and cytochrome c3 in energy production system. Arch. Microbiol. 125, 35–42. https://doi.org/10.1007/BF00403195

Van Niel, E.W.J., Gottschal, J.C., 1998. Oxygen consumption by Desulfovibrio strains with and without polyglucose. Appl. Environ. Microbiol. 64, 1034–1039. https://doi.org/10.1128/aem.64.3.1034-1039.1998

Van Niel, E.W.J., Pedro Gomes, T.M., Willems, A., Collins, M.D., Prins, R.A., Gottschal, J.C., 1996. The role of polyglucose in oxygen-dependent respiration by a new strain of Desulfovibrio salexigens. FEMS Microbiol. Ecol. 21, 243–253. https://doi.org/10.1016/S0168-6496(96)00060-8

Vita, N., Valette, O., Brasseur, G., Lignon, S., Denis, Y., Ansaldi, M., Dolla, A., Pieulle, L., 2015. The primary pathway for lactate oxidation in Desulfovibrio vulgaris. Front. Microbiol. 6. https://doi.org/10.3389/fmicb.2015.00606

Waite, D.W., Chuvochina, M., Pelikan, C., Parks, D.H., Yilmaz, P., Wagner, M., Loy, A., Naganuma, T., Nakai, R., Whitman, W.B., Hahn, M.W., Kuever, J., Hugenholtz, P., 2020. Proposal to reclassify the proteobacterial classes Deltaproteobacteria and Oligoflexia, and the phylum Thermodesulfobacteria into four phyla reflecting major functional capabilities. Int. J. Syst. Evol. Microbiol. 70, 5972–6016. https://doi.org/10.1099/ijsem.0.004213

Welsh, D.T., Lindsay, Y.E., Caumette, P., Herbert, R.A., Hannan, J., 1996. Identification of trehalose and glycine betaine as compatible solutes in the moderately halophilic sulfate reducing bacterium, Desulfovibrio halophilus. FEMS Microbiol. Lett. 140, 203–207. https://doi.org/10.1111/J.1574-6968.1996.TB08337.X

Zheng, Y., Kahnt, J., Kwon, I.H., Mackie, R.I., Thauer, R.K., 2014. Hydrogen formation and its regulation in Ruminococcus albus: Involvement of an electron-bifurcating [FeFe]-hydrogenase, of a non-electron-bifurcating [FeFe]-hydrogenase, and of a putative hydrogen-sensing [FeFe]-hydrogenase. J. Bacteriol. 196, 3840–3852. https://doi.org/10.1128/JB.02070-14

Zientz, E., Six, S., Unden, G., 1996. Identification of a third secondary carrier (DcuC) for anaerobic C4-dicarboxylate transport in Escherichia coli: roles of the three Dcu carriers in uptake and exchange. J. Bacteriol. 178, 7241–7247. https://doi.org/10.1128/JB.178.24.7241-7247.1996